Fish and Shellfish Immunology 90 (2019) 446–455

Contents lists available at ScienceDirect

Fish and Shellfish Immunology

journal homepage: www.elsevier.com/locate/fsi

Full length article

Adiponectin as inducer of inflammatory and apoptosis involving in immune defense in lamprey

Kejia Zhang[a,b,1], Zhao Tai[a,b,1], Qing Han[a,b,1], Yue Pang[a,b,**], Qingwei Li[a,b,*]

[a] College of Life Science, Liaoning Normal University, Dalian, 116081, China
[b] Lamprey Research Center, Liaoning Normal University, Dalian, 116081, China

A B S T R A C T

Adiponectin (APN) is an important cytokine secreted by fat cells that is responsible for regulating numerous biological functions. However, the APN gene in lamprey and its precise function remain unidentified. In this study, the full-length cDNA sequence of L-APN was cloned, and it encoded a protein of 267 amino acid residues with a globular domain. The results of immunohistochemistry and FACS assays showed that APN protein was distributed in multiple tissues. L-APN expression in the supraneural body (SB) and leukocytes was differentially upregulated in response to Gram-negative bacteria, Gram-positive bacteria and poly (I:C). The expression levels of inflammatory cytokines were upregulated, and a proapoptotic effect was stimulated in SB cells treated with recombinant APN. Furthermore, L-APN could inhibit cell proliferation and arrest cell growth in the G1 phase. In summary, the APN protein from the lamprey plays an important role in inhibiting cell proliferation, inducing the production of inflammatory cytokines and promoting cell apoptosis, and it is also involved in immune responses and immune defenses. Our data provide insights into the evolutionary origin of the structure and function of APN gene.

1. Introduction

It is now known that adipose tissue is a dynamic endocrine organ that secretes a number of biologically active proteins known as adipokines [1]. Adiponectin is one of several adipokines that circulates at a high concentration in the blood (3–30 μg/mL) as three oligomeric complexes [2,3]. Relatively low adiponectin expression is associated with various human metabolic diseases and some cancers [4]. The amino acid sequence of adiponectin is very similar to that of complement 1q factor (C1q). Interestingly, the crystal structure of the globular region from adiponectin shows a striking similarity to that of tumor necrosis factor-α (TNFα), despite dissimilar amino acid sequences https://en.wikipedia.org/wiki/Adiponectin [5]. Adiponectin plays important roles in fatty acid oxidation, hepatic gluconeogenesis, insulin sensitivity and chronic inflammation. Adiponectin also imparts antiatherogenic effects by upregulating AMP-activated protein kinase (AMPK) signaling and acting on the central nervous system to regulate food intake and body weight [6–8]. Therefore, adiponectin is a promising candidate for the development of drugs to treat obesity, insulin resistance, type 2 diabetes and other related metabolic diseases [9].

Lamprey is one of the two most ancient representatives of the vertebrate group, and thus, lamprey species are critical for exploring the biological evolution and origin of the immune system due to their unique evolutionary position [10,11]. The vertebrate immune system can eliminate exogenous pathogens and abnormal cells. In contrast to the broad body of knowledge on APN in jawed vertebrates, little is known about the existence and potential roles of APN in jawless vertebrates.

In this paper, we identified and characterized an adiponectin homolog from *Lampetra mori* Berg, designated L-APN. We revealed that L-APN plays prominent proinflammatory and proapoptotic roles and that it inhibits cell proliferation by inducing cell-cycle arrest. In addition, the potential roles of L-APN in the immune response and immune defense were also investigated. Based on these results, we propose that adiponectin serves as a tumor necrosis factor that facilitates efficient inflammation and apoptosis under immune defense conditions.

2. Materials and methods

2.1. Animals and cell culture

Adult lampreys (*Lampetra japonica*) were captured from the Tong River of China and kept in 4 °C water in a glass tank. Adult lampreys (200–220 g in weight, 49–52 cm in length) were anesthetized with 0.05% tricaine methanesulfonate (MS-222; 3-aminobenzoic acid ethyl ester, Sigma), which is an excellent and safe anesthesia, and blood was then collected by severing the tails of lampreys. Peripheral blood leukocytes were separated using Ficoll-Hypaque density centrifugation (density = 1.092 g/mL) [12]. The SB cells were isolated from the SB

* Corresponding author. College of Life Science, Liaoning Normal University, Dalian, 116081, China. Tel. +086 411 85827799.
** Corresponding author. Lamprey Research Center, Liaoning Normal University, Dalian, 116081, China.
E-mail addresses: pangyue@lnnu.edu.cn (Y. Pang), liqw@lnnu.edu.cn (Q. Li).
[1] These authors contributed equally to this work.

https://doi.org/10.1016/j.fsi.2019.04.045
Received 30 November 2018; Received in revised form 10 April 2019; Accepted 11 April 2019
Available online 16 April 2019
1050-4648/

tissue via 0.25% trypsin treatment. The handling of the lampreys and all of the experimental procedures were approved by the Animal Welfare and Research Ethics Committee of the Institute of Dalian Medical University (Permit Number: SYXK2004-0029). We performed the animal experiments at the Institute of Dalian Medical University. Lampreys (three in each group) were intraperitoneally injected with PBS (0.1 mL), *Vibro anguillarum*, *Aeromonas hydrophila*, *Vibrio splendidus*, *Vibro parahemolyticus*, *Micrococcus lysodeikticus*, *Vibro alginnolyficus* (approximately 1×10^7 in 0.1 mL of PBS), *S. aureus* (approximately 1×10^7 in 0.1 mL of PBS), or poly (I:C) (100 μg) [12].

MCF-7, HeLa and HepG-2 cells were maintained in RPMI 1640 medium (Sigma-Aldrich), and RAW264.7 cells were maintained in DMEM medium. Both media were supplemented with 10% fetal bovine serum, 100 U/mL penicillin and 100 mg/mL streptomycin (Gibco, Life Technologies). Cells were cultured in an incubator with 5% CO_2 at 37 °C.

2.2. Amino acid sequence and phylogenetic analyses

The novel APN homolog from lamprey was obtained via analysis of an expressed sequence tag (EST) cDNA library using the Basic Local Alignment Search Tool X (BLASTx) at the National Center for Biotechnology Information (NCBI). Total RNA was isolated from the supraneural body using Trizol (Invitrogen, USA), and the DNA was amplified using a High Fidelity PrimeScript™ RT-PCR Kit (TaKaRa Biotechnology, Dalian, China). The PCR primers were designed based on the ESTs of an APN homolog (Table 1). The PCR product was purified and cloned into the pMD19-T vector using a DNA ligation kit (TaKaRa, Japan) prior to DNA sequencing.

The amino acid sequence deduced from the L-APN gene sequence was analyzed using Bioedit, MEGA and NJ tools. The complete amino acid sequence alignments of various APN family members, including L-APN, were performed using Clustal X 1.83 and BioEdit with the default settings. The obtained results were converted into the MEGA format and imported into MEGA 5.05 to construct a phylogenetic tree using the neighbor-joining (NJ) method with 1000 bootstrapped replicates. Homology analysis of the APN sequences was performed using BLASTx from NCBI. Functional domain analyses of L-APN were also conducted using online tools at http://smart.embl-heidelberg.de.

2.3. Purification of the rL-APN protein and preparation of anti-L-APN antibodies (Abs)

The open reading frame (ORF) of the APN gene, which was flanked by *Eco*RI and *Hin*dIII restriction sites, was amplified and subcloned into the pCold I vector, which encodes a His tag. Recombinant APN was expressed in *RosettaBlue* competent cells induced with 1 mM isopropyl-1-thio-β-D-galactopyranoside (IPTG) for 24 h at 16 °C. The purification of recombinant L-APN was performed using a Ni-NTA His-bind column. To eliminate the possibility of contamination with bacterial factors, endotoxins were removed from the rL-APN protein with the GenScript ToxinEraser endotoxin removal kit (GenScript, China), and the endotoxin levels were confirmed to be below 10 EU/mL via the ToxinSensor Chromogenic LAL Endotoxin Assay kit (GenScript, China).

Two New Zealand white rabbits were first injected with purified rL-APN protein (400 μg/rabbit) mixed with complete Freund's adjuvant (CFA) (Sigma, USA) at a 1:1 ratio; next, they were subcutaneously injected with the protein (200 μg/rabbit) mixed with incomplete Freund's adjuvant. After 6 subsequent injections, repeating the immunizations at 1-week intervals, blood was drawn from the rabbit carotid artery, and the antibody was purified using Protein A (GenScript, USA). The antibody titer was determined via an enzyme-linked immunosorbent assay (ELISA). For western blotting, total lamprey serum protein was extracted and the protein concentrations were determined using a BCA Protein Assay Kit (Beyotime, China). A total of 500 ng of purified rL-APN and 80 μg of total protein from different lamprey tissues were then subjected to 12% SDS-PAGE and then transferred to nitrocellulose (NC) membranes. The membranes were blocked with 5% skim milk and incubated with the rabbit anti-L-APN Ab (1000-fold dilution) overnight at 4 °C, followed by incubation with horseradish peroxidase (HRP)-conjugated goat anti-rabbit IgG (5000-fold dilution). The membranes were developed using an enhanced chemiluminescence (ECL) substrate (Beyotime, China).

2.4. Quantitative real-time PCR (Q-PCR)

The extraction of leukocytes from the blood and supraneural body cells were performed as described previously [13]. Total RNA was extracted from each lamprey tissue sample using TRIzol (Invitrogen, USA), and the RNA was treated with DNase I (TaKaRa, China). Controls omitting the reverse transcriptase (No-RT) were prepared for each sample. Reverse transcription was performed as previously described. Q-PCR was conducted with the TaKaRa SYBR® PrimeScript™ RT-PCR Kit according to the manufacturer's protocol. Each reaction contained 1 × SYBR Premix Ex Taq, 10 mM concentrations of each primer, and 2 mL of cDNA (50 ng/mL) in a final volume of 25 mL. Amplification was performed in a TaKaRa PCR Thermal Cycler Dice Real Time System with the following parameters: initial denaturation at 95 °C for 30 s to activate the DNA polymerase, followed by 40 cycles of 5 s at 95 °C, 30 s at 60 °C, and 30 s at 72 °C. The specific primers for L-APN, L-IL-17, macrophage migration inhibitory factor (L-MIF), high mobility group box protein 1 (L-HMGB1), leucocyte cell-derived chemotaxin 2 (L-LECT2) for QPCR were designed and are shown in Table 1. Glyceraldehyde3-phosphate dehydrogenase (GAPDH) was used as an internal control. Each sample was analyzed in triplicate using the Thermal Cycler Dice Real Time System analysis software (TaKaRa, China). The

Table 1
Sequences of primer.

Spcecis	Gene Name	Primer (F/R)	Nucleotide sequence	Accession or Contig Number
Lamprey	L-APN (Full length)	Forward primer	5′-CTGTCCACACTGAACACTGCGAT-3′	MK681798
		Reverse primer	5′-CTCTTTTTCAAGGATGACTCGGC-3′	
	L-GAPDH (QPCR)	Forward primer	5′-AACCAACTGCCTGGCTCCT-3′	AY578058
		Reverse primer	5′-GTCTTCTGCGTTGCCGTGT-3	
	L-APN (QPCR)	Forward primer	5′-TCCTGGCAAGAATGGCGAGAAAG-3′	MK681798
		Reverse primer	5′-AGAGGAAGGTCACCAAAAACAGG-3′	
	L- IL-17 (QPCR)	Forward primer	5′-CTGGTTCTGAGACGCACGAA-3′	AB303391
		Reverse primer	5′-TGTCTCTAGGTCCGGCTTGTAAA-3′	
	L-MIF (QPCR)	Forward primer	5′-CGTAGGCTGGAACGGATCAAC-3′	AY280622
		Reverse primer	5′-CCACAAGGGTGGGAAAGGATT -3′	
	L-HMGB1 (QPCR)	Forward primer	5′-CCCGTCGGCTTTCTTCATC-3′	AEH59759
		Reverse primer	5′-TTCCACATCTCACCCAGTTTCTT -3′	
	L-LECT2 (QPCR)	Forward primer	5′-CCAACCGACAGTGCTGCAT-3′	MK716278
		Reverse primer	5′-TGTGTTTGTGGCCAGATCAT-3′	

specificity of the qPCR was validated by melting curve analysis.

RAW 264.7 cells were treated with 10 μg/mL rL-APN protein for 0 and 24 h, and LPS (1 mg/mL) was included as a positive control. Total RNA was extracted using the RNAiso reagent (Takara Bio, Shiga, Japan) according to the manufacturer's protocol. Total RNA (2 μg) was reverse transcribed using a Takara reverse transcriptase Kit (TaKaRa, China). Each sample was run in triplicate. The expression levels were determined using the standard curve method with respective cDNA fragments as standards. The level of GAPDH was used as an internal control. The primer sequences for the cytokines are also listed in Table 1.

2.5. Immunohistochemical staining and laser scanning confocal microscopy

Tissue samples were fixed and sectioned, and the tissue sections were then treated according to a previously reported method [14]. The sections were blocked with 10% normal goat serum for 3 h at room temperature and then incubated with the anti-L-APN polyclonal Ab at a 1/1000 dilution (0.6 μg/mL) for 3 h at room temperature, followed by addition of HRP-conjugated goat anti-rabbit IgG and rinsing with PBS. Normal rabbit IgG was used as a negative control. To confirm the staining specificity, some sections were stained with normal rabbit IgG or antibody that had been preabsorbed with recombinant L-APN. Subsequently, the slides were stained with diaminobenzidine (DAB) and counterstained with hematoxylin. Following dehydration, the sections were passed through successively diluted concentrations of xylene for 15 min each and then mounted in neutral resin.

Lamprey liver cells and supraneural body cells were trypsin digested and then washed with PBS. The cells were then fixed and permeabilized as previously described [13], followed by blocking with normal 10% donkey serum for 3 h and incubation with 4.8 μg/mL of anti-L-APN Abs (125-fold dilution) at 4 °C overnight. After the overnight incubation, the cells were washed with PBS and then incubated with Alexa Fluor 488-labeled donkey anti-rabbit IgG (500-fold dilution). Following washes with PBS, the cells were stained with 4′,6-diamidino-2-phenylindole (DAPI) (1000-fold dilution). The immunofluorescence was then visualized and captured with a Zeiss LSM 780 inverted microscope (Carl Zeiss, Inc.) and analyzed using Zeiss ZEN software. The cells were analyzed on a FACSCalibur flow cytometer (BD Biosciences) using an argon laser emitting at 488 nm. Cells incubated with normal rabbit IgG were used as isotype controls.

2.6. MTT assay

The effect of L-APN protein on cell viability was measured via MTT assays as described in a previous study [15]. MCF-7, HeLa, HepG-2, SB and liver cells were seeded in 96-well plates at a density of 2×10^4 cells per well and then incubated at 37 °C in culture medium. After 24 h, the cells were incubated with different concentrations of L-APN protein (10, 25 and 50 μg/mL) for 24 h as test condition. Each testing point included 3 wells. After incubation, a total of 50 μL of MTT solution (5 mg/mL) was added to each well, and the plates were incubated at 37 °C. After 3 h, the supernatant was discarded, and the formazan dye was dissolved in 200 μL of DMSO. The absorbance of each well was measured at 490 nm in a microplate reader to determine the formazan concentration, which is proportional to the number of live cells.

2.7. Caspase 3/7 apoptosis assay

First, 50 μL of caspase 3/7 substrate from the caspase 3/7 kit was added to 10 mL of assay buffer, according to the manufacturer's instructions. Myeloid cells were stimulated with 50 μg/mL of L-APN, and *cis*-diamine dichloroplatinum (CDDP) was used as a positive control. Next, 500 μL of caspase 3/7 activity detection reagent was added to each group, and the samples were mixed and incubated at room temperature for at least 1 h in the dark prior to flow cytometry analysis. The percentage of apoptotic cells were evaluated using a FACSCalibur flow cytometer (BD Biosciences, USA).

2.8. Annexin V-FITC/PI apoptosis assay

The supraneural body cells were incubated with 50 μg/mL rL-APN protein or treated with CDDP for 36 h. Afterwards, the cells were washed by PBS (4 °C) and 1 × binding buffer followed by the resuspension of the cell pellet in 100 μL of 1 × binding buffer. Next, 5 μL of Alexa Fluor 488 annexin V was added to the cell suspension, followed by incubation for 10 min in the dark at room temperature, according to the manufacturer's instructions. Propidium Iodide (PI) (5 μL) was added to the cell suspension, followed by 5 min of incubation in the dark at room temperature. Finally, 500 μL of PBS was added for flow cytometry analysis.

2.9. Cell cycle analysis by flow cytometry

MCF-7 cells were cultured in 60-mm plates at a density of 5×10^5 cells/well for 24 h. The next day, the MCF-7 cells were treated with 50 μg/mL L-APN protein. After 24 h of incubation, the cells were fully digested with pancreatic enzymes (25%) including EDTA to form a monocellular suspension. The cells were harvested, washed twice with phosphate-buffered saline (PBS) and fixed in 70% ethanol (in PBS) overnight at 4 °C. Next, the cells were washed twice and resuspended in PBS containing 0.1 mg/mL RNase (Sigma, USA). After incubation at 37 °C for 30 min, the cells were resuspended in PBS containing 50 μg/mL propidium iodide and analyzed using flow cytometry (BD). The DNA content of the stained cells was analyzed using CellQuest Software with a FACSCalibur flow cytometer (BD).

2.10. Statistical analysis

The statistical analyses were performed in GraphPad Prism. Each experiment in this study was performed in triplicate, and all experiments were repeated at least three times on separate occasions. The data are presented as the mean ± SD. Student's t-test was used to compare data between groups. All statistical tests included two-way analysis of variance. Statistical significance was accepted at p-values less than 0.05.

3. Results

3.1. Amino acid sequence analysis alignment of the L. mori Berg L-APN cDNA and phylogenetic analysis of the L-APN protein

We identified a fragment whose nucleotide sequence shared high homology with the human APN homolog. 3′- and 5′-RACE using primers designed based on this fragment resulted in the successful isolation of a full-length L-APN cDNA of 2202 bp. This cDNA consists of an 804-bp ORF that encodes 267 amino acid residues, a 70-bp 5′-untranslated region (UTR) and a 1328-bp 3′-UTR with a polyadenylation signal (Fig. 1A). Lamprey APN contains four distinct regions. The first region is a leading signal sequence for secretion outside the cell; next is a variable region that varies between species; the third region is a 59-amino collagen domain; and the last region consists of a globular domain with a striking similarity to the complement 1Q factor (C1Q) and structural similarities to tumor necrosis factor and collagens VIII and X (Fig. 1B). Sequence alignment of L-APN with the human APN gene revealed that it has 50–60% sequence homology with a conserved globular domain at the C-terminus of the protein, which plays a significant role in its bioactivity (Fig. 1C).

To investigate the evolutionary relationships between *L. mori* Berg APN and its counterparts, we used the neighbor-joining method to construct a phylogenetic tree of the gC1q domains of proteins that have both collagenous and gC1q domains. This analysis showed that L-APN is an orthologue of mammalian APN protein. L-APN should be placed

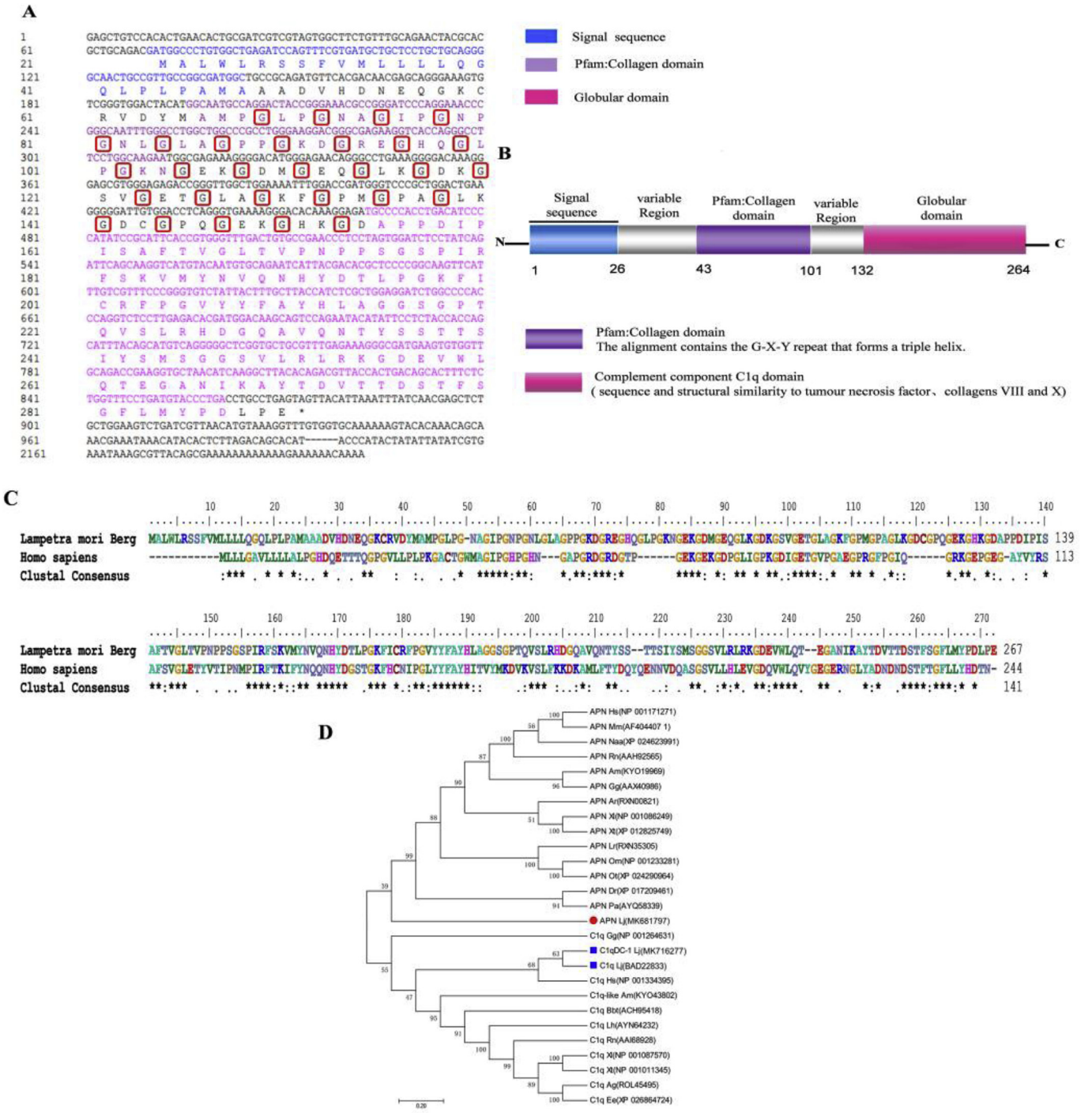

Fig. 1. Evolutionary analyses of L-APN. Multiple sequence alignment and phylogenetic analysis of L-APN. (A) Signal sequences are highlighted in blue; the collagenous domain in purple; the globular domain (which is contained in the complement component C1q domain) in pink; the 3′-and 5′-RACE in black. The functional domains of L-APN were predicted using the tool at http://smart.embl-heidelberg.de/. (B) Prediction of the conserved domains in L-APN. (C) Alignment of APN and C1q sequences from different vertebrate species. (D) Neighbor-joining tree for L-APN. An NJ tree was constructed using APN amino acid sequences. The numbers at the nodes indicate the bootstrap confidence values derived from 1000 replications. The bar (0.2) indicates genetic distance. The accession numbers of the amino acid sequences extracted from the NCBI protein database are shown in the figure. (For interpretation of the references to colour in this figure legend, the reader is referred to the Web version of this article.)

outside of the vertebrate clade, and it represents the most divergent APN subfamily protein in vertebrates. As shown in Fig. 1D, the L-APN, L-C1q and L-C1qDC-1 sequences are clustered separately at the bottom of the evolutionary tree. However, L-C1q and L-C1qDC are orthologues of mammalian C1q protein, following lower to higher evolutionary relationships.

3.2. Expression and purification of the rL-APN protein and antibody preparation and identification

To express recombinant L-APN in *RosettaBlue* (DE3) *E. coli* cells, a recombinant expression plasmid, pCold I-L-APN, was constructed. Amplification of the L-APN gene by PCR produced a single 804-bp DNA fragment encoding mature L-APN protein with a length of 267 amino

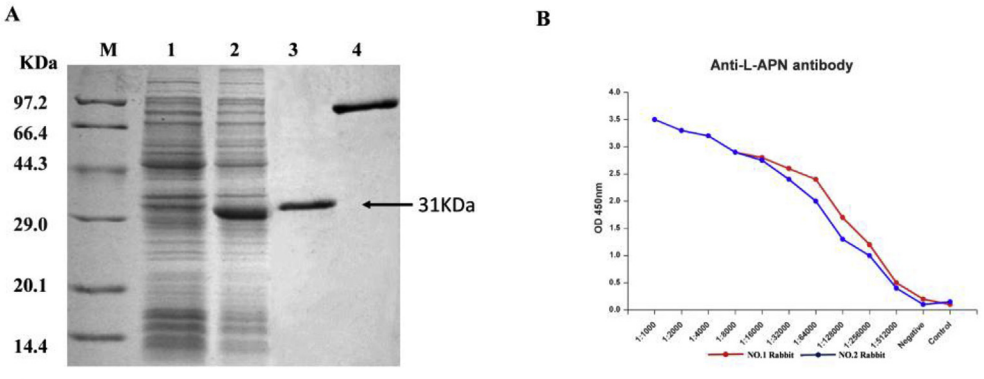

Fig. 2. Purification of rL-APN protein and Ab specificity analysis. (A) Analysis of rL-APN expression via SDS-PAGE. M, low molecular-weight protein marker; Lane 1, non-induced *RosettaBlue*/pCold I-L-APN cells; Lane 2, induced *RosettaBlue*/pCold I-L-APN cells; Lane 3, purified recombinant protein; Lane 4, BSA standard ampules 1 mg/mL (B) ELISA assay to assess the serum antibody titer from two rabbits. (C) Analysis of the specificity of the rabbit anti-L-APN polyclonal Abs by Western blot.

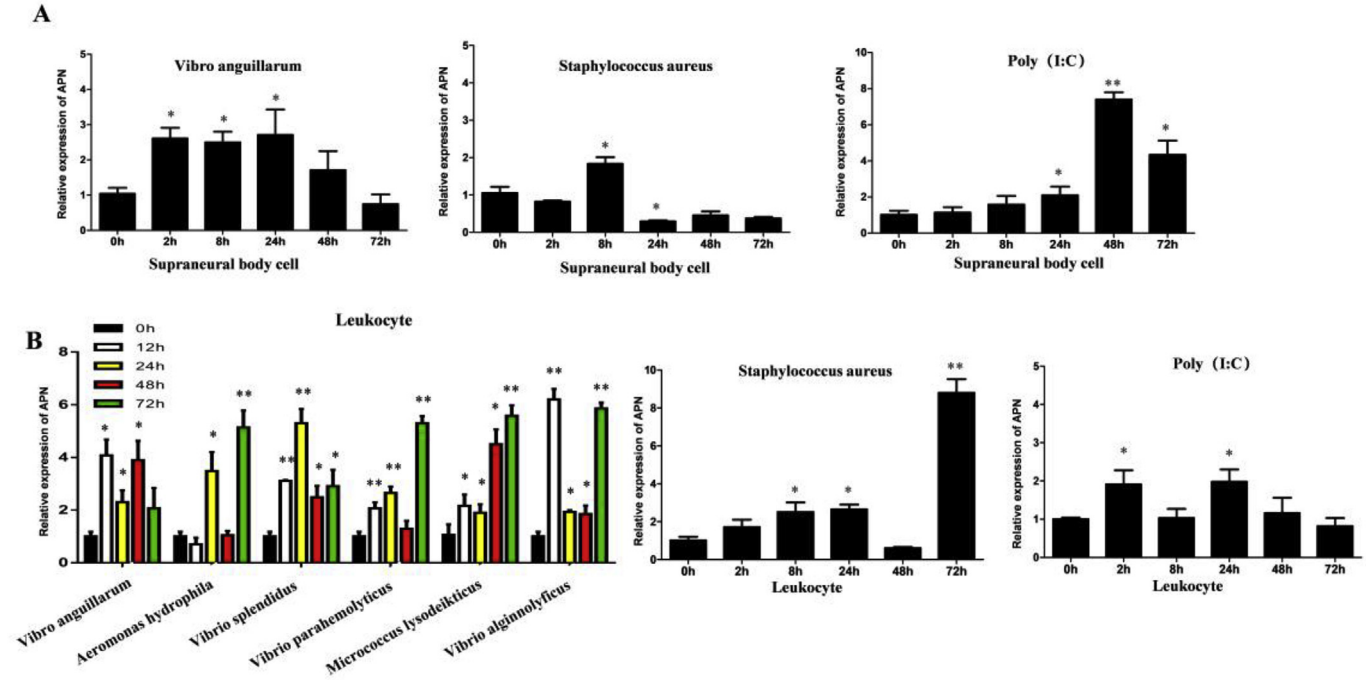

Fig. 3. The expression pattern of lamprey APN after bacterial and poly(I:C) challenge. (A) qRT-PCR analyses of the expression patterns of the L-APN gene in supraneural body cells after challenge with Gram-negative *Vibro anguillarum*, Gram-positive *S. aureus* and poly (I:C). (B) qRT-PCR analyses of the L-APN gene expression levels from leukocytes after stimulation with different bacteria and poly (I:C) for varying times. The results are presented as the fold-induction in mRNA abundance relative to that in samples from animals injected with PBS as determined via the $2^{-\triangle\triangle Ct}$ method from two parallel experiments performed in triplicate. The endogenous control for normalization was cytoplasmic gapdh. *p < 0.05 and **p < 0.01 versus the PBS control.

acids. Next, recombinant L-APN protein was expressed and purified as a His-tagged fusion protein using *RosettaBlue* cells. The purified rL-APN migrated as a single band in a 12% SDS-PAGE gel with a molecular mass of approximately 31 kDa (Fig. 2A). Rabbit anti-L-APN polyclonal antibody was generated through subcutaneous injection of New Zealand white rabbits with purified rL-APN protein over 8 weeks. The antibody titer in the anti-L-APN serum were determined via ELISA at different dilutions, and the titer was increased 512,000-fold over pre-immunization levels (preimmunized rabbit IgG was used as a negative control). The Ab specificity was confirmed through Western blot assays using recombinant L-APN protein and lamprey tissue samples. The results showed that the anti-L-APN antibody recognized native APN protein in liver and supraneural body tissues (Fig. 2B).

3.3. mRNA expression and distribution of L-APN in different lamprey tissues

The supraneural body (SB) and leukocytes are considered to be

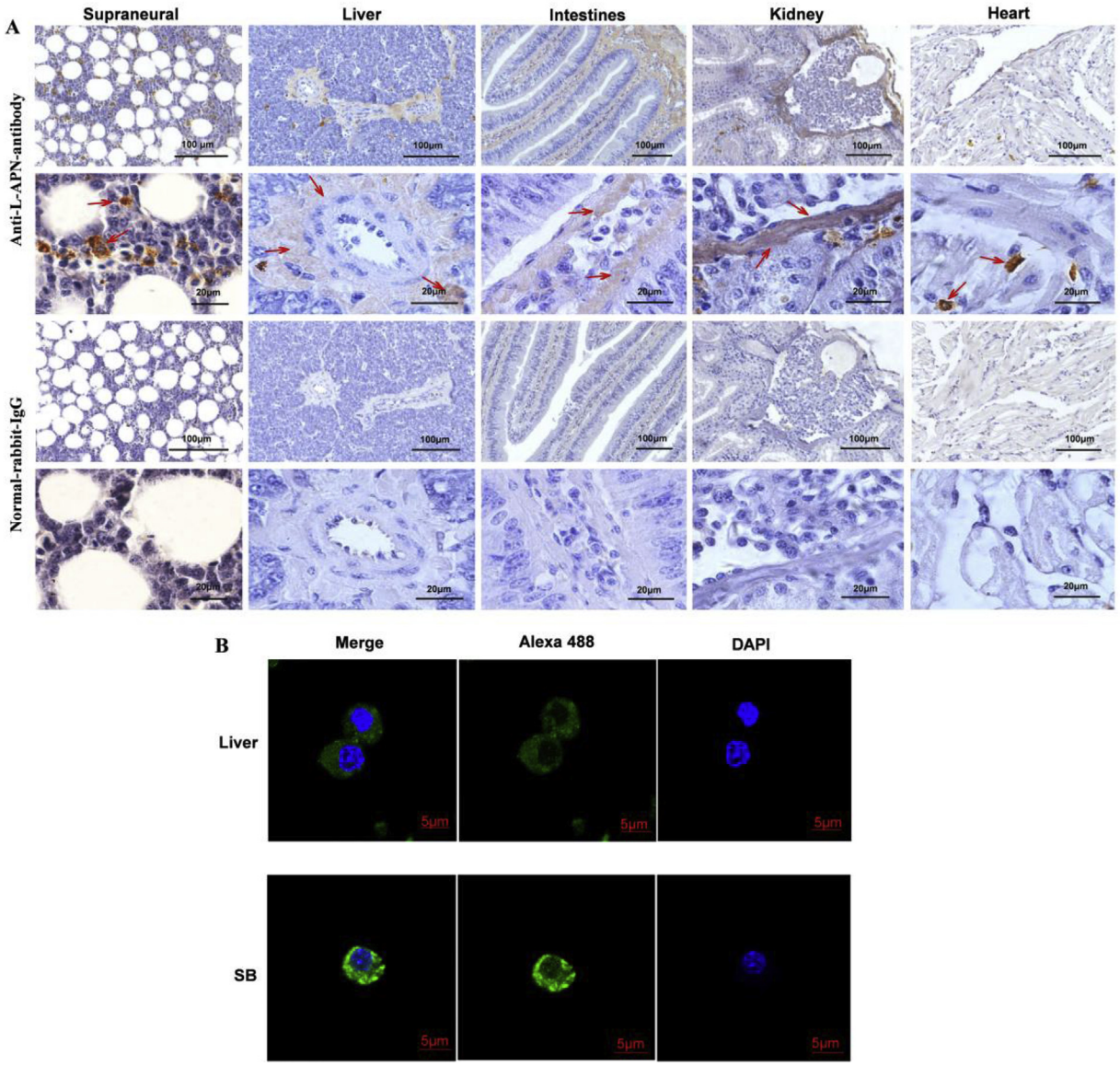

Fig. 4. The tissue distribution and cellular localization of L-APN. (A) Localization and distribution of the L-APN protein as observed by immunohistochemical staining. The tissue sections were incubated with L-APN rabbit polyclonal antibody (upper row). Normal rabbit IgG served as a negative control (bottom row). Scale bars: 100 μm and 20 μm. (B) Immunofluorescence localization of L-APN in lamprey liver cells and supraneural body cells. The primary antibody was the L-APN rabbit polyclonal antibody (200-fold dilution) and the secondary antibody was an Alexa Fluor 488-conjugated goat anti-rabbit IgG antibody (500-fold dilution). The cells were stained with DAPI. The immunofluorescence was visualized and captured using a confocal microscope (Carl Zeiss, Inc). Scale bar: 5 μm.

involved in the lamprey immune defense. To study the immunological significance of L-APN, real-time PCR analysis was performed using L-APN-specific primers. As shown in Fig. 3, the L-APN transcription levels in SB cells and leukocytes were significantly upregulated at different time points after challenge with a Gram-negative (G^-) bacterium, Gram-positive (G^+) bacteria and poly (I:C) (Fig. 3). After stimulation with Gram-positive bacteria, the APN transcription level in the leukocytes first increased and then decreased, and stimulation with Gram-negative bacteria resulted in a gradual increase (Fig. 3B). Its abundance in immune tissue and its responsiveness to bacterial challenge suggests that L-APN is a proinflammatory factor in the immune system.

In addition, the results of immunohistochemistry experiments revealed that L-APN protein is well expressed in the supraneural body and liver, to a lesser extent, in the intestines, kidneys and heart tissue of lamprey (Fig. 4A). Western blot results revealed that L-APN protein was mainly distributed in the supraneural body, liver, serum, intestine and kidney, GAPDH was used as a normalization reference (Fig. 2C). Furthermore, the intracellular localization of L-APN was examined by confocal laser-scanning microscopy, and preferential L-APN expression was observed in the cytoplasm of both SB and liver cells of the lamprey (Fig. 4B).

3.4. L-APN has potential proinflammatory and proapoptotic effects in lamprey cells

To confirm the proinflammatory the effect of L-APN in supraneural body cells, the expression levels of inflammatory molecules were further analyzed via real-time PCR using total RNA obtained from untreated or L-APN-treated supraneural body cells. The result confirmed that treatment with L-APN significantly increased the expression of HMGB1, an inflammatory cytokine factor in lamprey (Fig. 5A).

The caspase family plays a very important role in mediating apoptosis, with caspase-3 being a key molecule that functions in many apoptotic signaling pathways. Caspase-3 normally exists in the cytoplasm as a zymogen that is activated at an early stage during apoptosis; however, its activity is significantly lower in the late stage of apoptosis

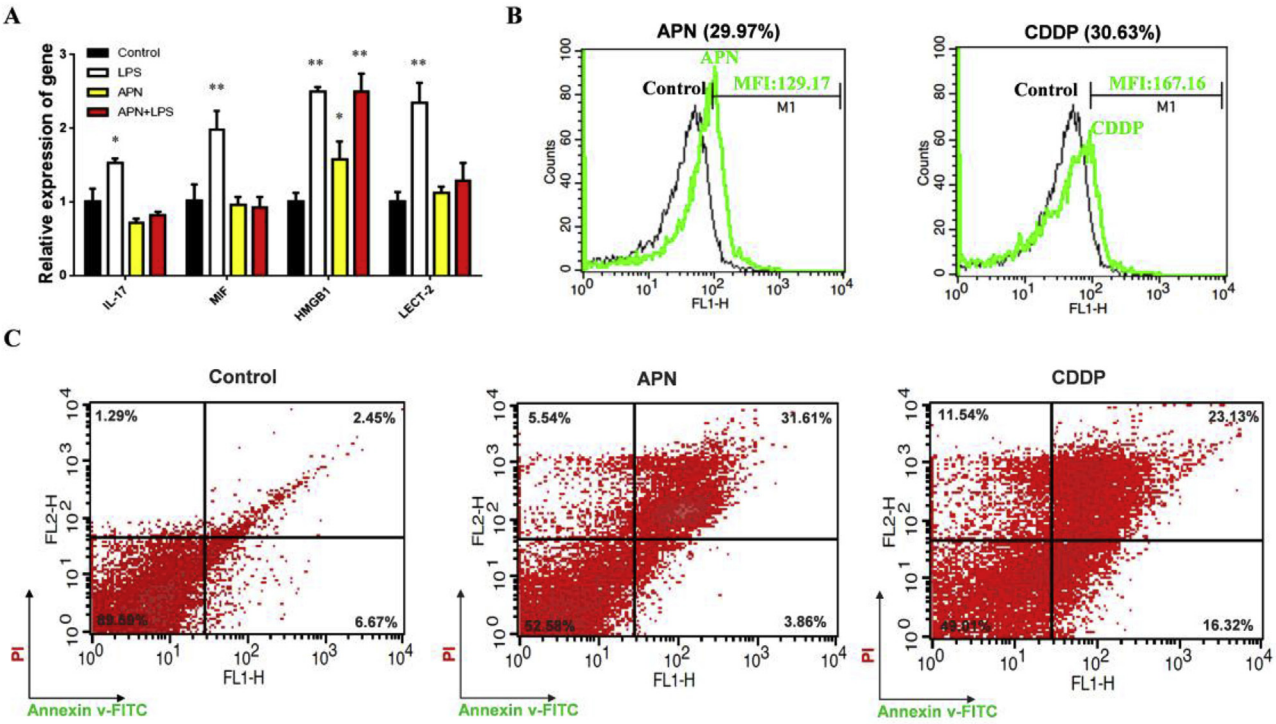

Fig. 5. The proinflammatory and pro-apoptotic roles of rL-APN in the supraneural body cells. (A) IL17, MIF, HMGB1 and LECT2 mRNA levels in lamprey SB cells were determined via real-time quantitative PCR after stimulation with PBS, LPS, rL-APN and a combination of LPS and rL-APN for 24 h. The endogenous control for the normalization was cytoplasmic gapdh. *$p < 0.05$ and **$p < 0.01$ versus the PBS control. (B) The apoptotic effect of rL-APN in supraneural body cells as assessed via flow cytometry. The supraneural body cells were incubated with 50 μg/mL rL-APN for 24 h, and cell death was detected via flow cytometry analysis with a caspase 3/7 apoptosis assay. (C) The apoptotic effect of rL-APN on supraneural body cells as assessed via flow cytometry. The supraneural body cells were incubated with 50 μg/mL rL-APN for 24 h, and cell death was detected by flow cytometry with Annexin V-FITC/PI staining.

and in dead cells. Apoptosis can be detected by measuring the caspase 3/7 abundance. Our results demonstrated typical morphological features of apoptosis in L-APN-treated supraneural body cells, and the apoptosis rates of SB cells were apparently increased compared with those of the negative control cells and the positive control cells, which were preincubated with 300 μM cisplatin (CDDP) (Fig. 5B).

Apoptosis has two distinct morphological and biochemical forms. Morphological changes in apoptotic cells, such as loss of plasma membrane asymmetry and attachment, plasma membrane blebbing, and condensation of the cytoplasm and nucleus, are always accompanied by several biochemical modifications [16]. Flow cytometry with Annexin V/PI double staining was employed to investigate the biochemical changes in L-APN-treated supraneural body cells. One of the earliest biochemical changes during apoptosis is a change in the level of phosphatidylserine (PS) exposed on the outer leaflet of the plasma membrane. Annexin V, a Ca^{2+}-dependent phospholipid-binding protein, interacts specifically and strongly with PS and can be used to detect apoptosis by indicating loss of plasma membrane asymmetry [17]. Our results confirmed the typical morphological features associated with apoptosis in L-APN-treated supraneural body cells, and the apoptosis rates of SB cells were apparently increased compared with those of the negative control cells and the positive control cells, which were preincubated with 300 μM cisplatin (CDDP) (Fig. 5C). In view of these observations, we suggest that L-APN plays important proinflammatory and apoptotic roles in lamprey.

3.5. L-APN affects tumor cell proliferation and cell cycle progression and enhances the release of inflammatory factors in RAW264.7 cells

The anti-proliferative effects of L-APN on various cell lines were evaluated using the MTT assay. This experiment is based on the capability of the NADP(H)-dependent cellular oxidoreductase enzyme to reduce the yellow tetrazolium dye MTT 3-(4,5-dimethylthiazol-2-yl)-2,5-diphenyltetrazolium bromide to the insoluble purple chemical formazan, whose level is proportional to the number of viable cells present. As shown in Fig. 6A, the viability of MCF-7, HeLa and HepG2 cells gradually decreased in a dose-dependent manner after 24 h of exposure to L-APN, indicating that L-APN had robust inhibitory effects on the proliferation of MCF-7, HeLa, and HepG2 cells. We also found that the different types of tumor cells had different sensitivities to L-APN. Furthermore, the MTT assay showed that rL-APN affected the viability of the lamprey SB cells and liver cells in a dose-dependent manner (10–50 μg/mL) (Paclitaxel (PTX) was used as a positive control).

Flow cytometry analysis was used to investigate whether the antiproliferative effect of L-APN on MCF-7 cells results from cell cycle arrest. The results confirmed that L-APN induced G1 phase arrest in MCF-7 cells. The proportion of G1-arrested cells was significantly increased after 48 h of treatment with concurrent decreases in the proportions of S and G2/M phase cells ($p < 0.05$). These results also indicate a significant increase in the proportion of apoptotic cells (Fig. 6C).

To examine whether the proinflammatory action of rL-APN was applicable to mammalian cells, we compared the mRNA expression levels of several inflammatory factors (TNF-α, IL-10, IL-6, IL-1β) in rL-APN-treated RAW264.7 cells. LPS treatment was used as the positive control. The results of quantitative real-time PCR assays revealed that rL-APN caused significant increases in the expression levels of TNF-α, IL-6, IL-10 and IL-1β. Furthermore, robust IL-1β expression was observed in RAW264.7 cells treated with a combination of rL-APN and LPS (Fig. 6D). Our data show proinflammatory effects of rL-APN in RAW264.7 cells, consistent with the results shown in Fig. 5A.

4. Discussion

For the past two decades, a great deal of research has been

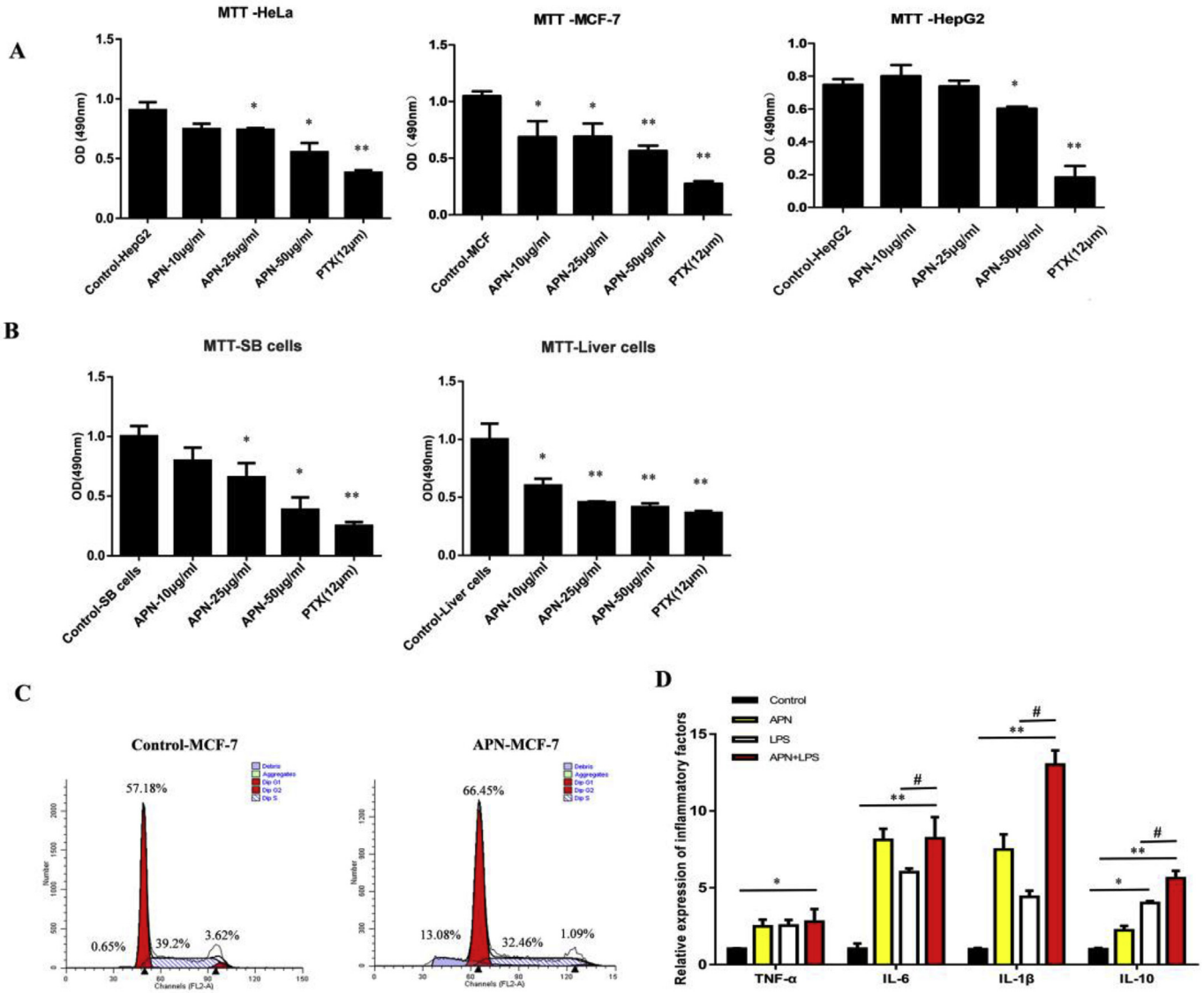

Fig. 6. Effects of rL-APN on tumor cells. (A) Inhibition of tumor cell proliferation after rL-APN treatment. The proliferative abilities of HeLa, MCF-7 and HepG2 cells were examined via MTT assays. The cells were treated with 10 μg/mL, 25 μg/mL and 50 μg/mL of rL-APN for 24 h *p < 0.05, **p < 0.01 compared with the results from the control group. (B) Reduced viability in SB and liver cells after rL-APN treatment. The viability of the SB and liver cells was examined via MTT assays. The cells were treated with 10 μg/mL, 25 μg/mL and 50 μg/mL of rL-APN for 24 h *p < 0.05, **p < 0.01 compared with the result of the control group. (C) Cell cycle progression was analyzed by flow cytometry in MCF-7 cells treated with rL-APN. The MCF-7 cells were cultured following 48 h treatment with 50 μg/mL of rL-APN. (D) qRT-PCR analysis of inflammatory molecule expression levels in RAW264.7 cells incubated with rL-APN. The TNF-α, IL-6, IL-1β and IL-10 mRNA levels were determined via real-time quantitative PCR in RAW264.7 cells after stimulation with PBS, LPS, rL-APN and a combination of LPS and rL-APN for 24 h. The endogenous control for the normalization was cytoplasmic gapdh. *p < 0.05 and **p < 0.01 versus PBS control, #p < 0.05 versus the LPS control.

published concerning APN, an abundant protein responsible for regulating numerous biological functions, including antioxidative, antinitrative, anti-inflammatory, and cardioprotective effects [18,19]. In this study, we identified the lamprey L-APN gene for the first time. The full-length cDNA includes an open reading frame of 804 bp that encodes a 29 kDa, 267-amino acid polypeptide that includes a 25-amino acid signal peptide. This protein includes a conserved structural element called a collagen domain. Due to the special status of lamprey, further evaluation of the L-APN molecule will provide important information regarding the function and evolution of the APN protein family.

Surprisingly, analysis of the peptide sequence of lamprey APN indicated that the lamprey protein was neither a collagen nor any known C1q homolog. Instead, it was a homolog of mammalian APN, despite containing a collagen-like sequence with many Gly-Xaa-Yaa repeats and a C-terminal globular C1q (gC1q) domain (Fig. 1A and B). L-APN shared 50% identity at the amino acid level with mammalian APN. Similar motifs are found in other proteins, such as type X collagen and C1q. Providing some insight into the origin and function of this crucial molecule, a phylogenetic analysis indicated that the L-APN protein appeared to be the most primitive form of its protein superfamily. Furthermore, the phylogenetic tree contained two clusters. The first cluster included the APN branches, and the second cluster included the C1q branches, progressing from lower to higher evolutionary relationships.

At present, little is known about the alteration of APN mRNA expression in lamprey in response to bacterial infection. As we known, adiponectin expression in mice was transiently increased after *Listeria monocytogenes* infection and then gradually decreased [20]. After V. anguillarum infection, the mRNA expression of adiponectin in ayu also slightly increased at first and then decreased [21]. To understand the modulation of L-APN expression in response to different microbial pathogens, the L-APN transcription levels in the supraneural body and

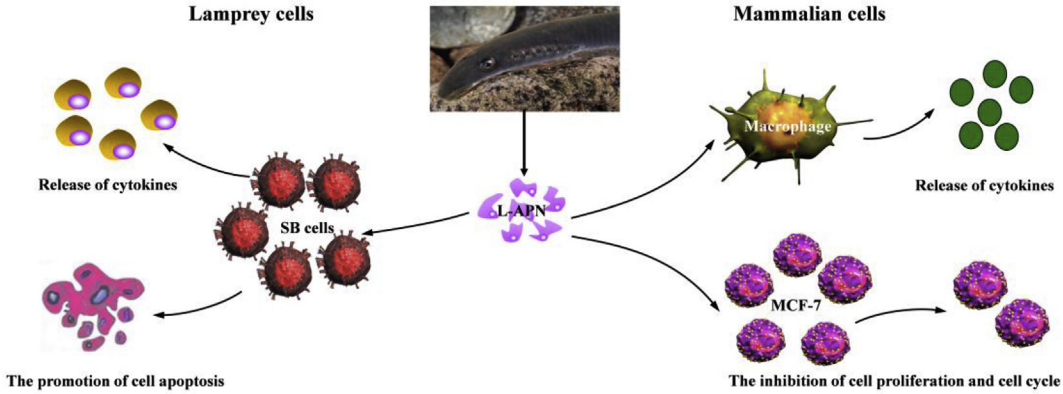

Fig. 7. Model of the functions of lamprey APN. Lamprey APN has various roles, inducing regulating cytokine release, inhibiting cell proliferation, arresting the cell cycle and promoting cell apoptosis. As an important immune molecule, lamprey APN may serve as a model for the biological activity of APN homologs in jawless vertebrates and may be involved in immune defense against bacterial and viral invasion.

leukocytes were measured at different time points after stimulation with Gram-positive bacteria, Gram-negative bacteria and poly (I:C) using qRT-PCR. In this study, our result showed the L-APN mRNA levels in the supraneural body and leukocytes were significantly upregulated and then gradually decreased upon stimulation with microbial pathogens. The expression of APN gene was up-regulated after *S. aureus* stimulation of myeloid cells in 8 h, indicating that the stimulation of different pathogens would cause difference in the upward trend (Fig. 3). The real-time PCR results showed that L-APN may be involved in the anti-bacterial immune response and that it might act rapidly to control mediators against infection. Collectively, the data suggest that the supraneural body and liver of lampreys act as barriers between the organism and its environment and take part in the innate immune response.

In rainbow trout, APN is abundantly expressed in the muscle and adipose tissue [22,23]. In ayu, adiponectin expression was detected in immune cells, although its highest level was detected in the adipose tissue [21]. To characterize the distribution of L-APN, we used immunohistochemical staining assays and intracellular immunofluorescence staining to analyze its expression pattern. The immunohistochemical results indicated that the highest levels of L-APN expression were in the supraneural body and liver. Moreover, the protein expression was concentrated in the vein vessels of the liver tissue (Fig. 4A). Immunohistochemical assays showed results identical to those of the Western blot analysis.

Adiponectin is the most abundant adipokine secreted from adipose tissue, and it has been reported to exert both anti- and proinflammatory effects in peripheral tissues [24]. Human APN is an important mediator of proinflammatory functions in viral diseases [25]. Elevated serum adiponectin levels have been found in association with systemic lupus erythematosus, cystic fibrosis, inflammatory bowel disease and rheumatoid arthritis [26–28]. To gain a better understanding of lamprey APN function, we performed experiments using lamprey and human cells. Our data confirmed that the expression levels of inflammatory cytokines in SB cells were upregulated following L-APN treatment. Thus, lamprey APN acts as a proinflammatory factor that induces the defense mechanism via an inflammatory response. Furthermore, the mRNA levels of inflammatory factors were upregulated in L-APN-treated RAW 264.7 cells. The results of flow cytometry analysis to assess apoptosis supported the predicted results, showing a significant increase in Annexin-V/PI binding following L-APN treatment in SB cells compared with that of untreated cells. The results of our apoptosis assays showed that L-APN has a proapoptotic role in SB cells in response to the intracellular immune response.

Adiponectin is an adipokine with insulin-sensitizing, anti-inflammatory, and anti-proliferative effects, while globular adiponectin induces a proinflammatory response in human astrocytic cells [29]. Adiponectin strongly upregulates lipid production in sebocytes and increases cell proliferation [30]. Furthermore, adiponectin induces dermal fibroblast proliferation and upregulates collagen production [31,32]. To date, no study has reported the effects of lamprey APN on human cancer cell lines. Therefore, the anti-proliferative effects and cell cycle regulation by APN in HeLa, MCF-7 and HepG2 cells were investigated in the present study. Our MTT assay results suggest that L-APN inhibits the proliferation of different human cancer cell types. Cell cycle arrest was analyzed by flow cytometry in MCF-7 and HeLa cells, the former of which were more sensitive to L-APN. L-APN induced cell cycle arrest in G1 phase in MCF-7 cells, while the effects in HeLa cells were not significant. However, flow cytometry analysis revealed that the percentage of debris in the treatment group was higher than that in the control group, suggesting that both cell types entered the early stage of apoptosis (Fig. 6C). Like mammalian APN, lamprey APN exhibits a wide range of biological activities. In future studies, the identification of an APN receptor-like gene in lamprey could cast light on its signaling pathway and other cooperative interactions. Adiponectin, as a regulator of the innate immune system, plays a role in the progression of inflammation and metabolic disorders in mammals. However, the roles of APN in fish are poorly understood. Three adiponectin fragments exist in ayu serum, but they have opposing roles in the regulation of monocyte/macrophage functions, specifically in controlling the up- and down-regulation of proinflammatory factors [21]. Are there different forms of lamprey APN with different functions? Further exploration is needed to address this question.

In summary, we identified an APN gene involved in the regulation of the lamprey innate immune response to pathogen infection. The APN mRNA expression levels were correlated with pathogen infection. The lamprey APN protein plays an important role in inhibiting cell proliferation, inducing the production of inflammatory cytokines and in promoting cell apoptosis, and it is also involved in immune responses and immune defenses. A summary of its functions is shown in Fig. 7. Collectively, our data on the lamprey APN gene provide the basis for structural comparison and functional studies between the APN homologs in lamprey and other species, and provide insight into the origin and evolution of the APN gene.

Declarations

Conflicts of interest

The authors declare that they have no competing interests.

Ethics approval and consent to participate

The animal experiments were performed in accordance with the

regulations of the Animal Welfare and Research Ethics Committee of the Institute of Dalian Medical University's Animal Care protocol (Permit Number: SCXK2008-0002).

Acknowledgments

This work was funded by the Chinese Major State Basic Research Development Program(973 Program; Grant2013CB835304); the Marine Public Welfare Project of the State Oceanic Administration (No.201305016); Chinese National Natural Science Foundation of China Grants (No.31170353, No.31202020, No.31772884); Science and Technology Innovation Fund Research Project (No.2018J12SN079); the Project of Department Of Ocean And Fisheries Of Liaoning Province (No.201805).

References

[1] S. Galic, J.S. Oakhill, G.R. Steinberg, Adipose tissue as an endocrine organ, Mol. Cell. Endocrinol. 316 (2) (2010) 129–139.
[2] K.S. Lam, A. Xu, Adiponectin: protection of the endothelium, Curr. Diabetes Rep. 5 (4) (2005) 254–259.
[3] T.S. Tsao, E. Tomas, H.E. Murrey, C. Hug, D.H. Lee, N.B. Ruderman, J.E. Heuser, H.F. Lodish, Role of disulfide bonds in Acrp30/adiponectin structure and signaling specificity. Different oligomers activate different signal transduction pathways, J. Biol. Chem. 278 (50) (2003) 50810–50817.
[4] Sungjin Ahn, Moonyoung Lee, 2-Formyl-komarovicine promotes adiponectin production in human mesenchymal stem cells through PPARc partial agonism, Bioorg. Med. Chem. 26 (5) (2018) 1069–1075.
[5] L. Shapiro, P.E. Scherer, The crystal structure of a complement-1q family protein suggests an evolutionary link to tumor necrosis factor, Curr. Biol. 8 (6) (1998) 335–338.
[6] N. Sucunza, M.J. Barahona, E. Resmini, J.M. Fernández-Real, W. Ricart, J. Farrerons, J. Rodríguez Espinosa, A.M. Marin, T. Puig, S.M. Webb, A link between bone mineral density and serum adiponectin and visfatin levels in acromegaly, J. Clin. Endocrinol. Metab. 94 (10) (2009) 3889–3896.
[7] A. Barseghian, D. Gawande, Bajaj M. Adiponectin and vulnerable atherosclerotic plaques, J. Am. Coll. Cardiol. 57 (7) (2011) 761–770.
[8] L. Ghazouani, A. Elmufti, I. Baaziz, I. Chaabane, Contribution of adiponectin polymorphisms to the risk of coronary artery disease in a North-African Tunisian population, J. Clin. Lab. Anal. 32 (7) (2018) e22446.
[9] S.M. Shimeld, P.C. Donoghue, Evolutionary crossroads in developmental biology: cyclostomes (lamprey and hagfish), Development 139 (12) (2012) 2091–2099.
[10] N. Ito, M. Mita, Y. Takahashi, A. Matsushima, Y.G. Watanabe, S. Hirano, S. Odani, Novel cysteine-rich secretory protein in the buccal gland secretion of the parasitic lamprey, Lethenteron japonicum, Biochem. Biophys. Res. Commun. 358 (1) (2007) 35–40.
[11] C.T. Amemiya, N.R. Saha, A. Zapata, Evolution and development of immunological structures in the lamprey, Curr. Opin. Immunol. 19 (5) (2007) 535–541.
[12] C. Li, D. Wang, X. Guan, S. Liu, P. Su, Q. Li, Y. Pang, HMGB1 from Lampetra japonica promotes inflammatory activation in supraneural body cells, Dev. Comp. Immunol. 92 (2019) 50–59.
[13] Y. Pang, S. Liu, Z. Zheng, X. Liu, Q. Li, Identification and characterization of the lamprey IRF gene, Immnol. Lett. 164 (2) (2015) 55–64.
[14] R. Xu, X. Song, P. Su, Y. Pang, Q. Li, Identification and characterization of the lamprey Flotillin-1 gene with a role in cell adhesion, Fish Shellfish Immunol. 71 (2017) 286–294.
[15] S. Lu, Y. Luo, P. Zhou, K. Yang, G. Sun, X. Sun, Ginsenoside compound K protects human umbilical vein endothelial cells against oxidized low-density lipoprotein-induced injury via inhibition of nuclear factor-κB, p38, and JNK MAPK pathways, J Ginseng Res 43 (1) (2019) 95–104.
[16] T. Mosmann, Rapid colorimetric assay for cellular growth and survival: application to proliferation and cytotoxicity assays, J. Immunol. Methods 65 (1–2) (1983) 55–63.
[17] M.A. Rahman, F. Ramli, H. Karimian, F. Dehghan, N. Nordin, H.M. Ali, S. Mohan, N.M. Hashim, Artonin E induces apoptosis via mitochondrial dysregulation in SKOV-3 ovarian cancer cells, PLoS One 11 (3) (2016) e0151466.
[18] M. Van Engeland, L.J. Nieland, F.C. Ramaekers, B. Schutte, C.P. Reutelingsperger, Annexin V-affinity assay: a review on an apoptosis detection system based on phosphatidylserine exposure, Cytometry 31 (1) (1998) 1–9.
[19] K. Robinson, J. Prins, B. Venkatesh, Clinical review: adiponectin biology and its role in inflammation and critical illness, Crit. Care 15 (2) (2011) 221.
[20] H. Sashinami, A. Nakane, Adiponectin is required for enhancement of CCL2 expression in adipose tissue during Listeria monocytogenes infection, Cytokine 50 (2) (2010) 170–174.
[21] H. Liu, X.J. Lu, J. Chen, Full-length and a smaller globular fragment of adiponectin have opposite roles in regulating monocyte/macrophage functions in ayu, Plecoglossus altivelis, Fish Shellfish Immunol. 82 (2018) 319–329.
[22] H. Kondo, R. Suga, S. Suda, R. Nozaki, I. Hirono, R. Nagasaka, G. Kaneko, H. Ushio, S. Watabe, EST analysis on adipose tissue of rainbow trout Oncorhynchus mykiss and tissue distribution of adiponectin, Gene 485 (2011) 40–45.
[23] H. Kondo, S. Suda, Y. Kawana, I. Hirono, R. Nagasaka, G. Kaneko, Hideki Ushio, Shugo Watabe, Effects of feed restriction on the expression profiles of the glucose and fatty acid metabolism-related genes in rainbow trout Oncorhynchus mykiss muscle, Fish. Sci. 78 (2012) 1205–1211.
[24] B. Venkatesh, I. Hickman, J. Nisbet, J. Cohen, J. Prins, Changes in serum adiponectin concentrations in critical illness: a preliminary investigation, Crit. Care 13 (4) (2009) R105.
[25] Zws Wan, D. Mah, S. Simtchouk, Globular adiponectin induces a pro-inflammatory response in human astrocytic cells, Biochem. Biophys. Res. Commun. 446 (1) (2014) 37–42.
[26] K. Karmiris, I.E. Koutroubakis, C. Xidakis, M. Polychronaki, T. Voudouri, E.A. Kouroumalis, Circulating levels of leptin, adiponectin, resistin, and ghrelin in inflammatory bowel disease, Inflamm Bowel Dis. 12 (2) (2006) 100–105.
[27] B.H. Rovin, H. Song, L.A. Hebert, T. Nadasdy, G. Nadasdy, D.J. Birmingham, C. Yung Yu, H.N. Nagaraja, Plasma, urine, and renal expression of adiponectin in human systemic lupus erythematosus, Kidney Int. 68 (4) (2005) 1825–1833.
[28] N. Moriconi, M. Kraenzlin, B. Muller, U. Keller, C.P. Nusbaumer, S. Stohr, M. Tamm, J.J. Puder, Body composition and adiponectin serum concentrations in adult patients with cystic fbrosis, J. Clin. Endocrinol. Metab. 91 (4) (2006) 1586–1590.
[29] M. Otero, R. Lago, R. Gomez, F. Lago, C. Dieguez, J.J. Gomez-Reino, O. Gualillo, Changes in plasma levels of fat-derived hormones adiponectin, leptin, resistin and visfatin in patients with rheumatoid arthritis, Ann. Rheum. Dis. 65 (9) (2006) 1198–1201.
[30] F. Duval, E. Dos Santos, H. Moindjie, V. Serazin, Adiponectin limits differentiation and trophoblast invasion in human endometrial cells, J. Mol. Endocrinol. 59 (3) (2017) 285–297.
[31] Y.R. Jung, J.H. Lee, K.C. Sohn, Y. Lee, Y.J. Seo, C.D. Kim, J.H. Lee, Adiponectin signaling regulates lipid production in human sebocytes, PLoS One 12 (1) (2017) e0169824.
[32] T. Ezure, S. Amano, Adiponectin and leptin up-regulate extracellular matrix production by dermal fibroblasts, Biofactors 31 (3–4) (2007) 229–236.